HOKKAIDO UNIVERSITY

Title	Theoretical investigations on hydrogen peroxide decomposition in aquo
Author(s)	Tsuneda, Takao; Taketsugu, Tetsuya
Citation	Physical chemistry chemical physics, 20(38), 24992-24999 https://doi.org/10.1039/c8cp04299c
Issue Date	2018-10-14
Doc URL	https://hdl.handle.net/2115/75761
Type	journal article
File Information	aper.pdf

Hokkaido University Collection of Scholarly and Academic Papers : HUSCAP

Theoretical investigations on hydrogen peroxide decomposition in aquo

Takao Tsuneda[1,2*] and Tetsuya Taketsugu[2]

[1]*Fuel Cell Nanomaterials Center, University of Yamanashi, Kofu 400-0021, Japan and*

[2]*Department of Chemistry, Faculty of Science,*

Hokkaido University, Sapporo 060-0810, Japan

Abstract

Hydrogen peroxide (H_2O_2) decomposition mechanisms under the absence and presence of iron ions in aqueous solution, which contain no OH radical formations, are theoretically determined. Calculating the oxygen-oxygen bond dissociation energies of H_2O_2, we confirmed that the OH radical formation requires spin-forbidden transitions. Instead, we tested an H_2O_2 dimer-based decomposition mechanism and found that this mechanism provides reasonable barrier heights with $52 \sim 62$ kcal/mol, which are close to the experimental activation energy. We next calculated the oxygen-oxygen bond dissociation of H_2O_2 coordinating to the iron ion hydration complex in order to explore the H_2O_2 decomposition under the presence of iron ions. Surprisingly, we found that a monovalent iron ion complex provides no reaction barrier to dissociate H_2O_2, in contrast to the ferrous (Fe^{2+}) and ferric (Fe^{3+}) ion complexes accompanying very high barriers. Following this result, we determined the subsequent oxygen formation mechanism of the monovalent iron ion complex and found that this mechanism needs a hydrogen bond network around H_2O_2 to proceed at room temperature. We, therefore, conclude that the H_2O_2 decomposition under the presence of iron ions is driven by the electron transfer to the iron ion hydration complex and proceeds by hydrogen transfers in the hydrogen bond network around H_2O_2.

I. INTRODUCTION

Hydrogen peroxide (H_2O_2) decomposition is frequently used as an efficient method for testing the durability of materials. For many materials, H_2O_2 is known as the main cause for the degradation, as found in, e.g., proton exchange membranes of fuel cells under the operation. Metal ions such as divalent iron (ferrous) and divalent manganese ions are well-known to decompose H_2O_2.[1,2] In Fenton test,[3] these ions are, therefore, used with H_2O_2 as reagents for degrading materials. Hydroxyl (OH) radicals have been taken as the main species for the decomposition in aqueous solution:

$$H_2O_2 \rightarrow 2OH, \tag{1}$$

$$H_2O_2 + OH \rightarrow HO_2 + H_2O, \tag{2}$$

$$2HO_2 \rightarrow H_2O_2 + O_2. \tag{3}$$

The ferrous ion-induced H_2O_2 decomposition has also been interpreted to proceed through the OH radical production. Haber and Weiss experimentally suggested an H_2O_2 decomposition mechanism by ferrous cation (Fe^{2+}):[4]

$$Fe^{2+} + H_2O_2 \rightarrow Fe^{3+} + OH + OH^-, \tag{4}$$

$$Fe^{2+} + OH \rightarrow Fe^{3+} + OH^-, \tag{5}$$

$$H_2O_2 + OH \rightarrow HO_2 + H_2O, \tag{6}$$

$$HO_2 + H_2O_2 \rightarrow O_2 + H_2O + OH. \tag{7}$$

Since the pKa value of HO_2 in Eq. (6) is 4.88,[5] HO_2 is considered to dissociate proton to produce O_2^- in neutral water, i.e.,

$$HO_2 \rightarrow H^+ + O_2^-. \tag{8}$$

The reaction of HO_2 and OH radicals is, therefore, often included in the mechanism as an O_2 formation process, i.e.,

$$OH + HO_2 \rightarrow O_2 + H_2O. \tag{9}$$

Moreover, Barb et al. replaced Eq. (7) with the following equations in another Fe^2-induced decomposition mechanism:[6,7]

$$Fe^{2+} + HO_2 \rightarrow Fe^{3+} + HO_2^-, \tag{10}$$

$$Fe^{3+} + HO_2 \rightarrow Fe^{2+} + H^+ + O_2. \tag{11}$$

In total, these equations are expressed as

$$2Fe^{2+} + 3H_2O_2 \rightarrow 2Fe^{3+} + 2OH^- + 2H_2O + O_2. \quad (12)$$

Based on this equation, the Fenton test[3] has been explained to produce OH radicals, which decompose H_2O_2. Note, however, that the lifetime of OH radicals is known to be only 10^{-7} s (100 ns) in aqueous solution, though it is 1 ms in gas phase. The lifetime in aquo is too short to initiate the degradation of polymer membranes. It is, therefore, reasonable to consider that there is another reaction pathway to decompose H_2O_2 without producing OH radicals.

Prior to the OH radical-production mechanism, Bray and Gorin experimentally proposed another H_2O_2 decomposition mechanism proceeding through the production of divalent iron oxide cation (FeO^{2+}):[8]

$$Fe^{2+} + H_2O_2 \rightarrow FeO^{2+} + H_2O, \quad (13)$$

$$FeO^{2+} + H_2O_2 \rightarrow Fe^{2+} + O_2 + H_2O. \quad (14)$$

However, FeO^{2+} had not been considered to play a significant role in the H_2O_2 decomposition for many years, because it appears to be too inactive to degrade materials. Baerends and coworkers theoretically investigated this FeO formation mechanism in the following equations:[9]

$$[(H_2O)_5Fe(H_2O_2)]^{2+} \rightarrow [(H_2O)_4Fe(OH)_2]^{2+} + H_2O, \quad (15)$$

$$[(H_2O)_4Fe(OH)_2]^{2+} \rightarrow [(H_2O)_5FeO]^{2+}. \quad (16)$$

These equations contain no OH radical formation, and instead, require the hydrogen transfer between oxygen atoms. In the present calculations, this hydrogen transfer provides a very high barrier height, which is inconsistent with the original result,[9] as mentioned later. Note also that they studied no subsequent mechanism after the FeO formation. Cannot this FeO formation mechanism substitute for the OH radical mechanism in the ferrous ion-induced H_2O_2 decomposition?

A recent experimental study shows that FeO is produced in the H_2O_2 decomposition and OH radicals hardly contribute to the H_2O_2 decomposition. Enami et al. performed a mass spectroscopy experiment of aqueous microjet containing iron(II) chloride ($FeCl_2$) for selectively observing low-concentrated compounds produced at aqueous interfaces with very short time scale ($< 5 \times 10^{-5}$ s).[10] As a result, they found that the H_2O_2 decomposition

reactions at the interfaces proceed 1,000 $\sim$ 10,000 times faster than those in aquo. Their results also indicate that the Fe^{2+} ion-induced H_2O_2 decomposition takes place as follows:

1. OH radicals hardly contribute to the decomposition, because an OH radical scavenger (tertiary butanol, t-BuOH) hardly affects the mass spectra,

2. FeO and Fe^{3+} are produced in the decomposition, because the mass spectrum peaks corresponding to these species appear, and

3. H_2O_2 may replace with a coordinated H_2O to initiate the decomposition, because the decomposition reaction rate is very fast at the interfaces.

These conclusions disprove conventional H_2O_2 decomposition mechanisms including OH productions and also indicate the significance of the decomposition mechanism through the FeO formation. As far as we know, the H_2O_2 decomposition reaction pathway through the FeO formation is not yet theoretically revealed. Elucidating this H_2O_2 decomposition mechanism will advance the understanding of the catalytic reactions by metal clusters.

In this study, H_2O_2 decomposition mechanisms are theoretically revealed for the reactions under the presence or absence of iron ions following the recent experimental findings. The theoretical calculations assumed that the iron ion-induced decompositions are driven by the replacement of a coordinated H_2O with H_2O_2 and contain the FeO formation without OH radical productions.

II. COMPUTATIONAL DETAILS

Calculations have been performed using the hydrated H_2O_2 monomer and dimer models, hydrated with 2, 4, 6, and 8 water molecules, and the hydrated iron ion model, in which $[Fe(H_2O_2)(H_2O)_5]^{n+}$ complex for $n = 1$ and 2 is used with two additional hydration H_2O molecules (Fig. 1). These model structures are determined by maximizing the number of hydrogen bonds and then selecting the minimum energy geometries in the several similar isomers. For these models, reactant, product and transition state (TS) calculations have been carried out to construct the reaction energy diagrams by the Kohn-Sham calculations[11,12] using the long-range correction[13,14] of Becke 1988 exchange[15] plus Lee-Yang-Parr correlation[16] (LC-BLYP) functional (the only parameter $\mu = 0.33$[17]). Note that the high reliability

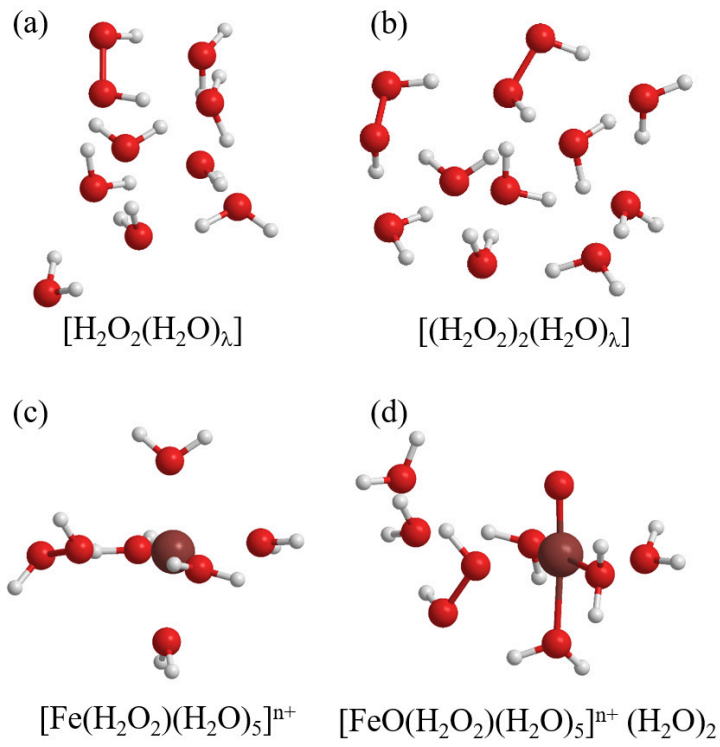

FIG. 1: Calculation models of (a) hydrated H_2O_2 monomer with λ hydration water molecules ($[(H_2O_2)_2(H_2O)_\lambda]$), (b) hydrated H_2O_2 dimer with λ hydration water molecules ($[(H_2O_2)_2(H_2O)_\lambda]$), (c) iron ion ($Fe^{n+}$) hydration complexes with λ coordinating water molecules ($[Fe(H_2O_2)(H_2O)_5]^{n+}$), and (d) iron oxide ion (FeO^{n+}) hydration complexes with λ coordinating water molecules and two additional water molecules ($[FeO(H_2O_2)(H_2O)_5]^{n+}(H_2O)_2$).

of this method has been confirmed in the previous calculations of related systems: e.g., the H_2O_2-induced degradation of hydrated Nafion membrane[18] and H_2O_2 decomposition by triphenylphosphine oxide.[19] The cc-pVDZ basis set[20,21] was used for H and O atoms and LANL2DZ effective core potential basis set[22] was employed for Fe atom. As a solvent effect, the polarizable continuum model[23] of water has been included. Transition state calculations have been performed by the quadratic synchronous transit method[24,25] using several initial structures for finding out the minimum energy pathways. The intrinsic reaction coordinate (IRC) calculations[26] have also been performed by the predictor-corrector integrator method[27,28] for all the TS structures to confirm the correctness of these TS structures. In the O-O dissociation calculations of H_2O_2, the stability conditions for spin-restricted Kohn-Sham calculations are attached to switch to the spin-unrestricted ones for spin-unstable

electronic states in order to avoid the instability of single-configurational DFT calculations for bond dissociations.[29,30] The Gaussian 09 suite of program[31] has been used to perform all of the LC-BLYP calculations. All of the optimized structures have been checked to ensure that they yield positive, real frequencies. The calculated IRCs have been analysed using GaussView 5.0.8.[32]

III. RESULTS AND DISCUSSION

A. H_2O_2 decomposition mechanism without metal ions

First, we explored the H_2O_2 decomposition mechanism without metal ions in aqueous solution. The OH radical formation mechanism, $H_2O_2 \rightarrow 2OH$, has been the most accepted H_2O_2 decomposition mechanism,[33–37] because the dissociation energy of H_2O_2 into OH radicals is evaluated as about 50 kcal/mol (e.g., 54.8 kcal/mol for H_2O_2 with no explicitly-bonded H_2O molecules in aqueous solution in the present calculation), while this energy is close to the experimentally-evaluated activation energy of the H_2O_2 decomposition without metal ions in aqueous solution, 47.8 kcal/mol.[34,35,38] Figure 2 illustrates the O-O dissociation potential energy curves for the hydration numbers λ = 0, 2, 4, 6, and 8 with the solvent effect. As shown in the figure, the O-O dissociations asymptotically approach the dissociation energies independently of the hydration numbers, in aqueous solution. Note, however, that the produced OH radicals rapidly recombine to form H_2O_2 under the hydrogen bond network, if the O-O dissociation proceeds with maintaining the singlet state. Actually, no subsequent potential energy curves is given for the longer O-O distances than 3 Å, because H_2O_2 is reproduced for the long O-O distances by hydrogen transfers in the hydrogen bond networks. Therefore, the spin multiplicity should be switched to the triplet state to maintain OH radicals. Though this spin flip takes place by spin-orbit transfers, it essentially needs very long time to proceed for such light atoms. We, therefore, consider that H_2O_2 is usually immediately recovered even if OH radicals are produced by the O-O dissociations.

Regardless of the presence or absence of OH radicals, the H_2O_2 decomposition stoichiometrically requires two H_2O_2 molecules, as shown in Eqs. (1) $\sim$ (3) and in Eqs. (13) $\sim$ (14). Considering the instability of OH radicals, it is, therefore, reasonable to assume that the H_2O_2 decomposition takes place by the association of H_2O_2 molecules. Figure 3 shows the

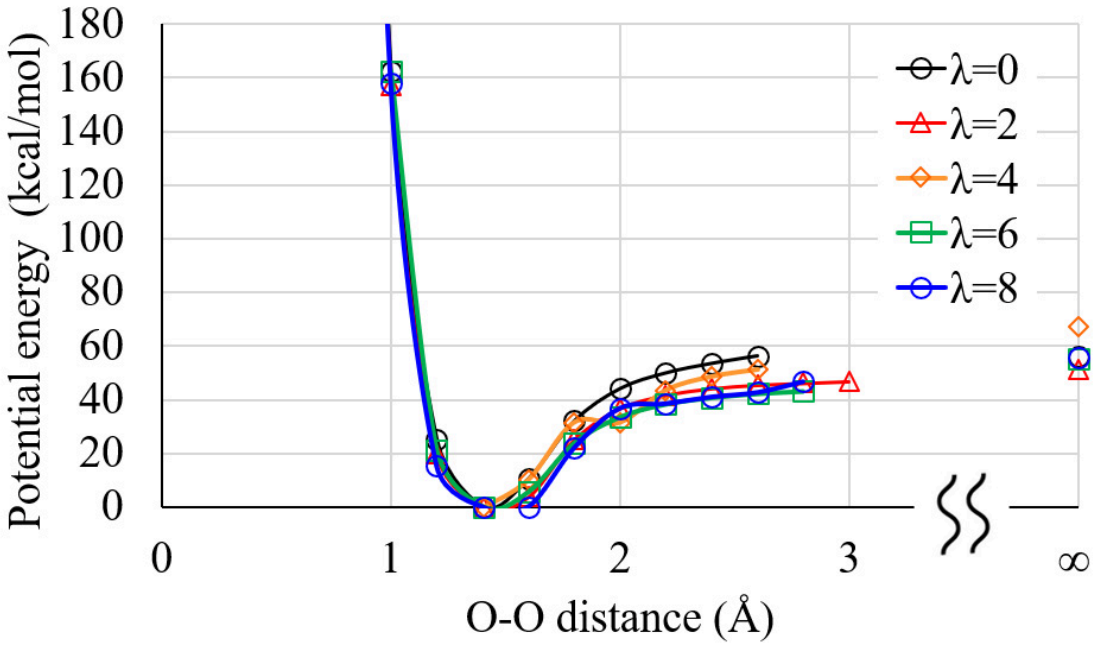

FIG. 2: Potential energy curves of the O-O dissociation of H_2O_2 to OH radicals for the explicit hydration numbers λ = 0, 2, 4, 6, and 8 in aqueous solution. The spin-restricted Kohn-Sham calculations are performed under the stability condition for switching to the spin-unrestricted ones.[29,30] LC-BLYP/cc-pVDZ is used with the solvent effect of the polarizable continuum model of water. The minimum potential energies are set to be zero. The dissociation limit energies, which are calculated by equally dividing the hydrated H_2O_2 such as $H_2O_2(H_2O)_{2\lambda} \rightarrow 2OH(H_2O)_\lambda$, are also shown at the infinite O-O distance.

reaction energy diagrams of the decomposition of the hydrated H_2O_2 dimer for the hydration numbers $\lambda = 0$, 2, 4, 6, and 8. For comprehension, the H_2O_2 dimer structures of $\lambda = 0$ (no explicitly-coordinated hydration water molecule) are shown for five reaction steps, though they are different from those of other hydration numbers except for the synthetic species (see Fig. S1 of the supporting information): H_2O_3 (OHOHO) radical is produced in the first step and O_2 and H_2O are synthesized in the second step. Note that this OHOHO radical is different from HOOOH radical, which is also considered to produce O_2 with small reaction barrier (8 kcal/mol in our previous calculation[19]). These radicals may be distinguished in the infrared spectrum study due to the difference in the vibrational spectrum peaks for 2500 $\sim$ 3200 cm^{-1} (see Fig. S2 of the supporting information). The figure indicates that the reaction barrier energies (52 $\sim$ 62 kcal/mol) are close to the dissociation energies, which are

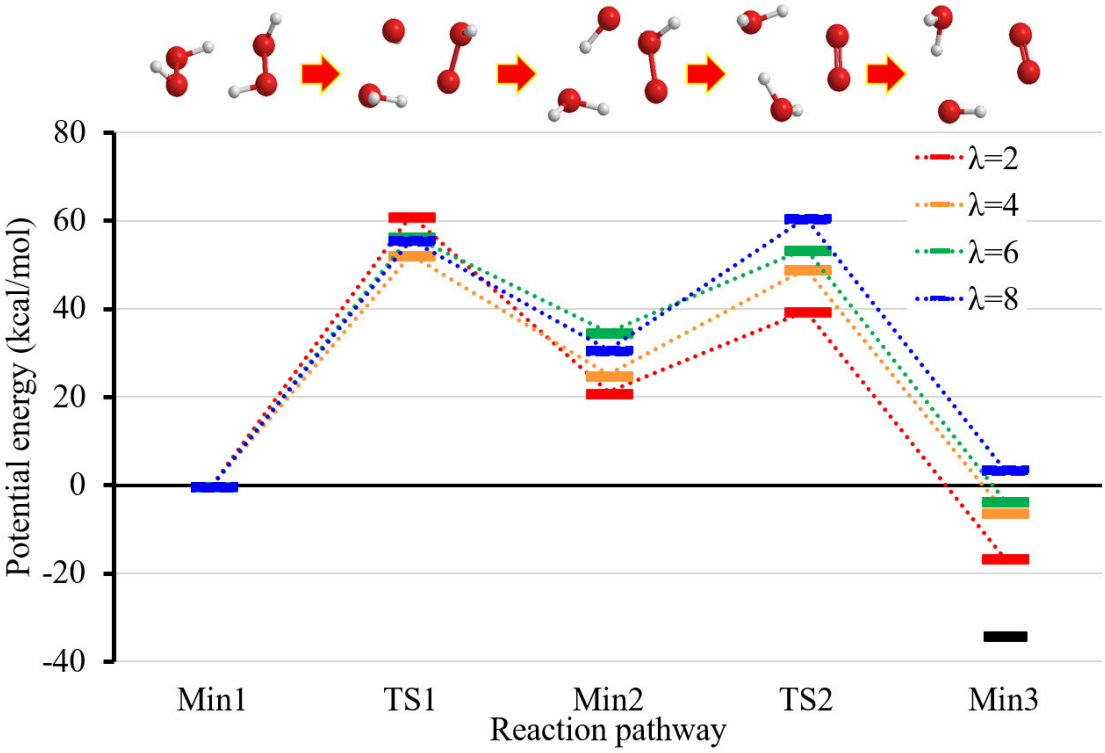

FIG. 3: Reaction diagram of H_2O_2 decomposition reaction, i.e., $2H_2O_2 \rightarrow O_2 + 2H_2O$, under the absence of metal ions in aqueous solution. LC-BLYP/cc-pVDZ is used with the solvent effect of the polarizable continuum model of water. Zero-point vibrational corrections are included. The molecular structures of the reaction processes are also shown for the complex with no water molecule. For Min3, the potential energy of the triplet state for $\lambda = 8$ is also shown as a black bar.

shown in Fig. 2, and are much smaller than the dissociation barrier heights of the $H_2O_2 \rightarrow$ 2OH reaction in aqueous solution mentioned above. The barrier energies tend to increase as the hydration number increases except for $\lambda = 2$ of Min1, while the intermediate (Min2) and final (Min3) products are destabilized as the hydration number increases except for $\lambda = 8$ of Min2. This is because both TSs and products contain neutral radicals such as OOH and O_2, which are unstable in aqueous solution. It may be questionable that this reaction pathway provides only the singlet state energies, though O_2 molecule has the ground triplet state. However, we consider that the real decomposition reaction also proceeds only through the singlet states. This is because the spin-forbidden spin-orbit transition probabilities from the singlet to triplet states are usually very small for such light and low-spin systems. The figure also shows that the H_2O_2 decomposition reaction is evaluated to be endothermic for

$\lambda = 8$. This result is also related to the spin-forbidden transitions, because O_2 molecule is finally produced to be the ground triplet state. The triplet state energy of Min3 is shown for $\lambda = 8$ as a black bar in Fig. 3. As clearly shown in the figure, this reaction is exothermic for the production of the triplet O_2 molecules even for $\lambda = 8$. We would emphasize that the above results are consistent with the experimental observations showing that H_2O_2 is hardly decomposed without metal ions in aqueous solution. Therefore, we conclude that H_2O_2 is decomposed by this mechanism under the absence of metal ions in aqueous solution.

B. FeO hydration complex formation mechanism

Next, we address the H_2O_2 decomposition mechanism under the presence of iron ions in aqueous solution. For exploring the decomposition mechanism, it is interesting to focus on the formation of the iron oxide (FeO) hydration complex. Baerends and coworkers explained that the $Fe^{IV}O$ hydration complex is formed in the following two steps:[9]

1. The O-O bond dissociation of H_2O_2 coordinating to the ferrous ion hydration complex proceeds to form OH radicals coordinating to the tetravalent iron ion hydration complex: i.e.,

$$[Fe^{II}(H_2O_2)(H_2O)_5]^{2+} \rightarrow [Fe^{IV}(OH)_2(H_2O)_4]^{2+} + H_2O, \tag{17}$$

   and

2. the FeO hydration complex is then formed from the OH radicals coordinating to the tetravalent iron ion hydration complex: i.e.,

$$[Fe^{IV}(OH)_2(H_2O)_4]^{2+} \rightarrow [Fe^{IV}O(H_2O)_5]^{2+}. \tag{18}$$

They suggested that steps 1 and 2 require very low barriers with only 6 and 2 kcal/mol, respectively, both of which are too low to inhibit the H_2O_2 decomposition proceeding at room temperature. We first explored the FeO formation mechanism on the basis of this study.

As a result, we found that the FeO hydration complex is formed in one step and that this step requires much higher reaction barriers for the ferrous ion hydration complex. Figure 4 displays the calculated potential energy curves of the O-O bond dissociation for two types

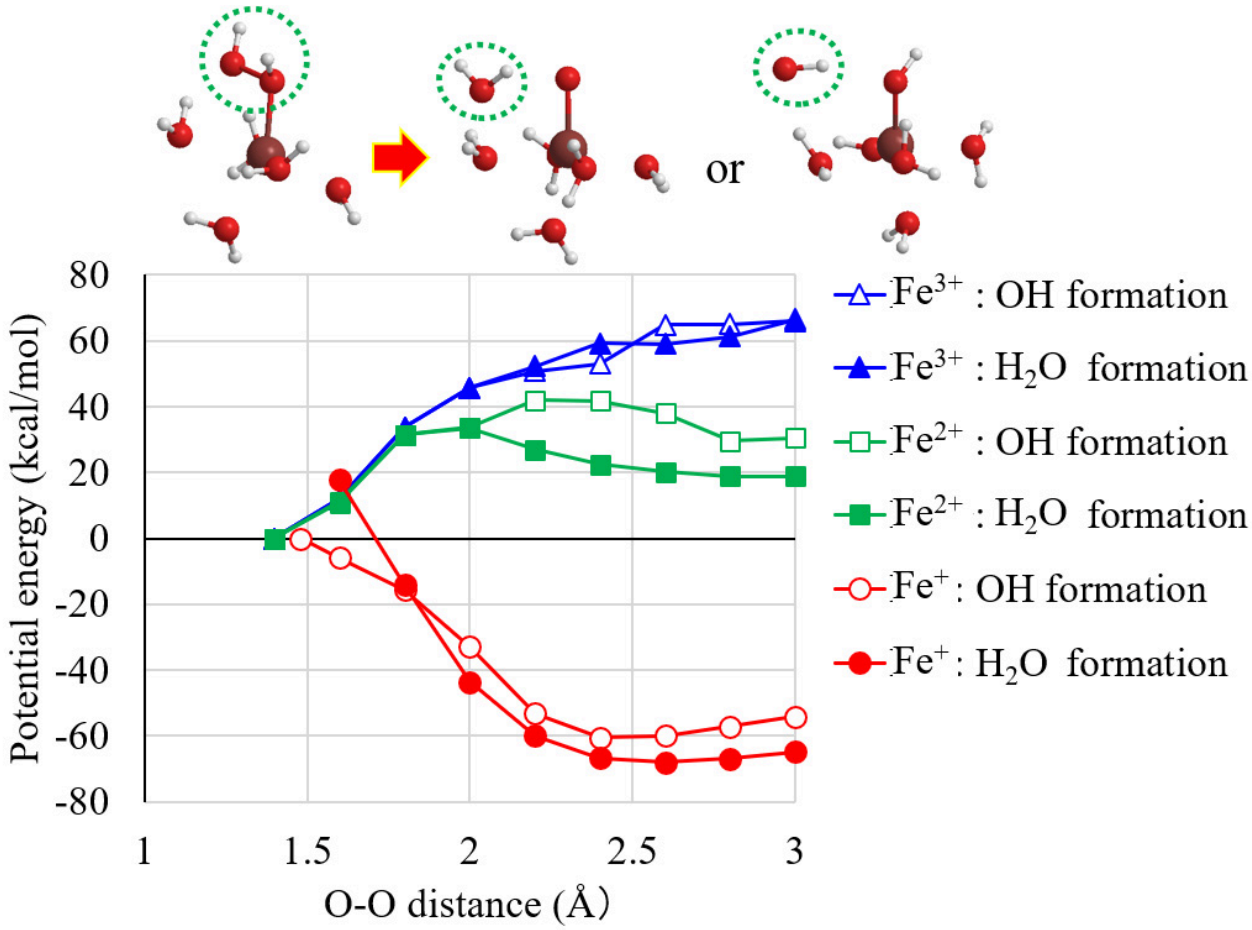

FIG. 4: Potential energy curves of the O-O bond dissociation of H_2O_2, which is coordinated to the iron ion hydration complexes in $[Fe(H_2O_2)(H_2O)_5]^{n+}$, for the valence of $n = 1$, 2, and 3. LC-BLYP/cc-pVDZ/LanL2DZ is used with the solvent effect of the polarizable continuum model of water. The dotted green circles indicate the H_2O_2 molecule and formed H_2O molecule and OH radical.

of the O-O dissociations: OH and H_2O formations. The OH formation type of the reaction corresponds to the above-mentioned first step: i.e.,

$$[Fe(H_2O_2)(H_2O)_5]^{n+} \rightarrow [Fe(OH)_2(H_2O)_4]^{n+} + H_2O. \tag{19}$$

On the other hand, the H_2O formation type corresponds to the integration of the first and second processes: i.e.,

$$[Fe(H_2O_2)(H_2O)_5]^{n+} \rightarrow [FeO(H_2O)_5]^{n+} + H_2O. \tag{20}$$

As the figure clearly shows, for the ferrous (Fe^{2+}) ion hydration complex, the H_2O formation type gives a high reaction barrier ($\sim$ 34 kcal/mol), while the OH formation type provides a higher barrier height ($\sim$ 40 kcal/mol). This is obviously inconsistent with the experimental results showing that O_2 is rapidly produced in H_2O_2 solution under the presence of ferrous ions. We also examined ferric (Fe^{3+}) ion hydration complex, because this ion is also experimentally detected[10] and there is an experiment measuring the decomposition rate.[39] As a result, we found that the barrier heights increase to more than 65 kcal/mol, which are higher than the barrier heights of the O-O dissociation of H_2O_2 without metal ions in Fig. 2. These results indicate that the FeO complex is rapidly formed by neither ferrous nor ferric ion hydration complexes at room temperature.

Monovalent iron ion hydration complex, i.e., $[Fe(H_2O_2)(H_2O)_5]^+$, is, therefore, examined as a FeO formation species. As far as we know, this complex has never been assumed to be a decomposition catalyst, because monovalent iron (Fe^+) ion is essentially unstable. Note that we assume not the production of Fe^+ ions but the electron transfer to the ligand molecules of the H_2O_2-coordinated ferrous ion hydration complex. This assumption is supported by an experimental evidence that the ferrous ion chelate complex with an electron-donating citrate acid is much more susceptible to oxidation than $[Fe(H_2O)_6]^{2+}$ complex.[40,41] The production of ferric ions also implicitly supports this assumption, because an electron must be generated to produce ferric ions from ferrous ions: i.e.,

$$2[Fe(H_2O)_6]^{2+} \rightarrow [Fe(H_2O)_6]^{3+} + [Fe(H_2O)_6]^{+}. \tag{21}$$

Figure 4 shows that the OH formation type provides no barrier for the monovalent iron ion hydration complex. This indicates that H_2O_2 is rapidly decomposed into OH radicals after the electron transfer to the ferrous ion hydration complex, as seen in the experiments. This result strongly suggests that the electron transfer to H_2O_2 coordinating to the ferrous ion complex is a precursory process of the H_2O_2 decomposition.

Figure 4 also indicates that H_2O formation provides higher barrier for the short O-O distance, though it gives a more stable potential energy. Considering that the OH radical from the dissociated H_2O_2 would form H_2O through the hydrogen bond network, we arranged two H_2O molecules around H_2O_2 to maximize the number of hydrogen bonds and optimized the geometry of the complex. We, consequently, found that the dissociated OH radical forms H_2O with no reaction barrier to produce the $Fe(OH)_2$ hydration complex in a similar way

to the first reaction process of Baerends et al.[9] in Eq. (17), i.e.,

$$[\mathrm{Fe^{I}}(\mathrm{H_2O_2})(\mathrm{H_2O})_5]^+ \rightarrow [\mathrm{Fe^{III}}(\mathrm{OH})_2(\mathrm{H_2O})_4]^+ + \mathrm{H_2O}, \tag{22}$$

As mentioned in Sec. III C, we found that the subsequent FeO^+ hydration complex formation from the $[Fe(OH)_2]^+$ hydration complex, i.e.,

$$[\mathrm{Fe^{III}}(\mathrm{OH})_2(\mathrm{H_2O})_4]^+ \rightarrow [\mathrm{Fe^{III}O}(\mathrm{H_2O})_5]^+, \tag{23}$$

requires the reaction barrier of 16.5 kcal/mol, which is considered to proceed at room temperature, when H_2O_2 is coordinated to the complex. We, therefore, conclude that the $Fe(OH)_2^+$ hydration complex is first produced from the O-O dissociation of H_2O_2, and then, the FeO^+ hydration complex is formed by the transformation of the $Fe(OH)_2^+$ complex, and finally, FeO^{2+} hydration complex is produced by losing an electron.

How are the monovalent iron ion hydration complex produced in the solution of the ferrous ion hydration complex? For iron ions in aqueous solution, Marcus exemplified a ferrous-ferric exchange reaction,

$$\mathrm{Fe^{2+}(aq)} + \mathrm{Fe^{3+}(aq)} \rightleftharpoons \mathrm{Fe^{3+}(aq)} + \mathrm{Fe^{2+}(aq)}, \tag{24}$$

as a typical electron transfer system in inorganic electrochemistry and developed a guiding theory for this exchange reaction.[42] This exchange reaction is a rare event, because it needs 0.1 s to proceed at equilibrium.[43] Note, however, that in chemical kinetics, this small reaction rate comes from the identity of the reactant and product. The present reaction is considered to proceed by the disproportion reaction of the ferrous ion hydration complex, i.e.,

$$2[\mathrm{Fe^{II}}(\mathrm{H_2O})_6]^{2+} \rightleftharpoons [\mathrm{Fe^{III}}(\mathrm{H_2O})_6]^{3+} + [\mathrm{Fe^{I}}(\mathrm{H_2O})_6]^+. \tag{25}$$

and then, the monovalent iron complex is rapidly oxidized to FeO hydration complex, i.e.,

$$[\mathrm{Fe^{I}}(\mathrm{H_2O_2})(\mathrm{H_2O})_5]^+ \rightleftharpoons [\mathrm{Fe^{III}O}(\mathrm{H_2O})_5]^+ + \mathrm{H_2O}. \tag{26}$$

This reaction is considered to mainly proceed when H_2O_2 is coordinated to the ferrous ion hydration complex, because the monovalent ion complex is essentially less stable than the ferrous and ferric ion complexes: i.e., for Eq. (25),

$$[\mathrm{Fe^{II}}(\mathrm{H_2O})_6]^{2+} + [\mathrm{Fe^{II}}(\mathrm{H_2O_2})(\mathrm{H_2O})_5]^{2+} \rightleftharpoons [\mathrm{Fe^{III}}(\mathrm{H_2O})_6]^{3+} + [\mathrm{Fe^{I}}(\mathrm{H_2O_2})(\mathrm{H_2O})_5]^+. \tag{27}$$

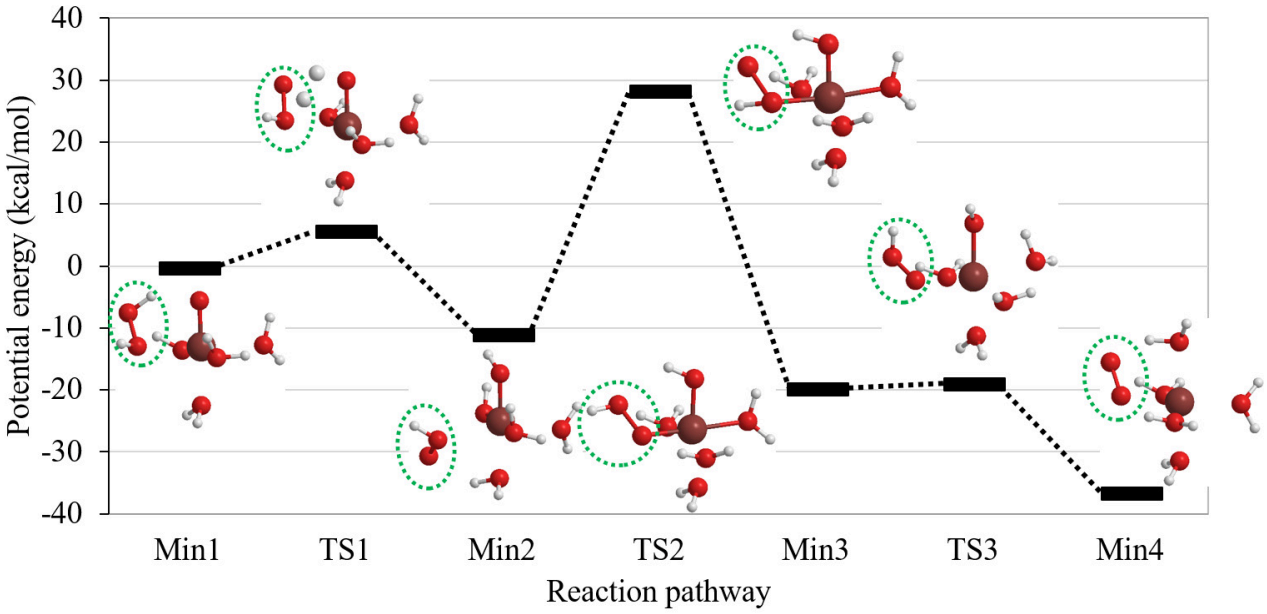

FIG. 5: O_2 formation mechanism of the H_2O_2-coordinated FeO^+ ion hydration complex with no additional H_2O molecules, i.e., $[FeO(H_2O_2)(H_2O)_4]^+$. LC-BLYP/cc-pVDZ/LanL2DZ is used with the solvent effect of the polarizable continuum model of water. Zero-point vibrational corrections are included. The potential energy of the reactant complex (Min1) is set to be zero. The dotted green circles indicate the H_2O_2 molecules and their decomposed fragments.

Since the concentration of the monovalent ion complex is reduced as a consequence of Eq. (26), the disproportion reaction in Eq. (25) kinetically proceeds rightward. This is contrasting to the identical reaction in Eq. (24), which is considered to be driven by environmental fluctuations from an energetical viewpoint.[43] In addition, the products of these reactions, FeO and Fe^{3+} hydration complexes, are consistent with the experimental result,[10] as mentioned in Sec. I.

C. O_2 formation mechanism from H_2O_2-coordinated FeO hydration complex

Following the very low reaction barrier of the FeO^+ hydration complex formation, it is meaningful to explore the subsequent O_2 formation mechanism from the monovalent iron ion hydration complex. We first examined the O_2 formation mechanism from the hydration complex with no additional hydration water molecule, i.e., $[FeO(H_2O_2)(H_2O)_4]^+$. Figure 5 illustrates the calculated reaction energy diagram of the O_2 formation mechanism. As shown

in the figure, a high barrier (39.3 kcal/mol) is given for the hydrogen transfer between the oxygen atoms of H_2O_2 in the second process (Min2 $\rightarrow$ Min3):

$$[Fe(OH)(OHO)(H_2O)_4]^+ \rightarrow [Fe(OH)(OOH)(H_2O)_4]^+, \tag{28}$$

while low barriers are provided for the first and third processes: 9.2 and 4.0 kcal/mol, respectively. Though this barrier is lower than those of the decomposition without metal ions (52 $\sim$ 62 kcal/mol), it is too high to be consistent with the experimental results showing the rapid O_2 formation at room temperature. We considered that this high barrier comes from the neglect of the hydrogen bond network around H_2O_2, because hydrogen transfers frequently occur in the hydrogen bond networks.

We have, therefore, added two hydration water molecules to the FeO^+ hydration complex, i.e.,

$$[FeO(H_2O_2)(H_2O)_6]^+ \rightarrow [Fe(OH)_2(H_2O_2)(H_2O)_5]^+ \rightarrow [Fe(H_2O)_7O_2]^+, \tag{29}$$

in order to model the hydrogen bond network between the coordinated H_2O_2 and surrounding H_2O molecules. Figure 6 illustrates the reaction energy diagram of the O_2 formation. As shown in the figure, the highest barrier is given for the first step (Min1 $\rightarrow$ Min2) as 14.0 kcal/mol, which is much lower than the barrier of the complex with no additional water molecule (39.3 kcal/mol). This low barrier is consistent with the experimentally-observed rapid H_2O_2 decomposition reaction under the presence of iron ions. This indicates that the hydrogen bond network around H_2O_2 significantly contributes to the H_2O_2 decomposition. Actually, the reaction energy diagram shows that hydrogen transfers mostly proceed through the hydrogen bond network. Note that the produced O_2 in this mechanism (Min6) is also considered to have the singlet state, similar to that in the decomposition mechanism without metal ions in Fig. 2. We, therefore, optimized the sextet state of Min6, which must contain the triplet state of O_2, and found that it becomes -18.8 kcal/mol more stable than the quartet state of Min6, which must contain the singlet state of O_2. As discussed in Sec. III A, we, however, consider that the decomposition reaction proceeds only through the singlet states due to the small spin-orbit transition probabilities. We would emphasize that this mechanism is clearly consistent with the recent experimental result,[10] in which OH radicals hardly contribute to the O_2 formation reaction, FeO and Fe^{3+} are produced from the Fe^{2+} hydration complex, and H_2O_2 is first replaced with a coordinated H_2O. We, therefore,

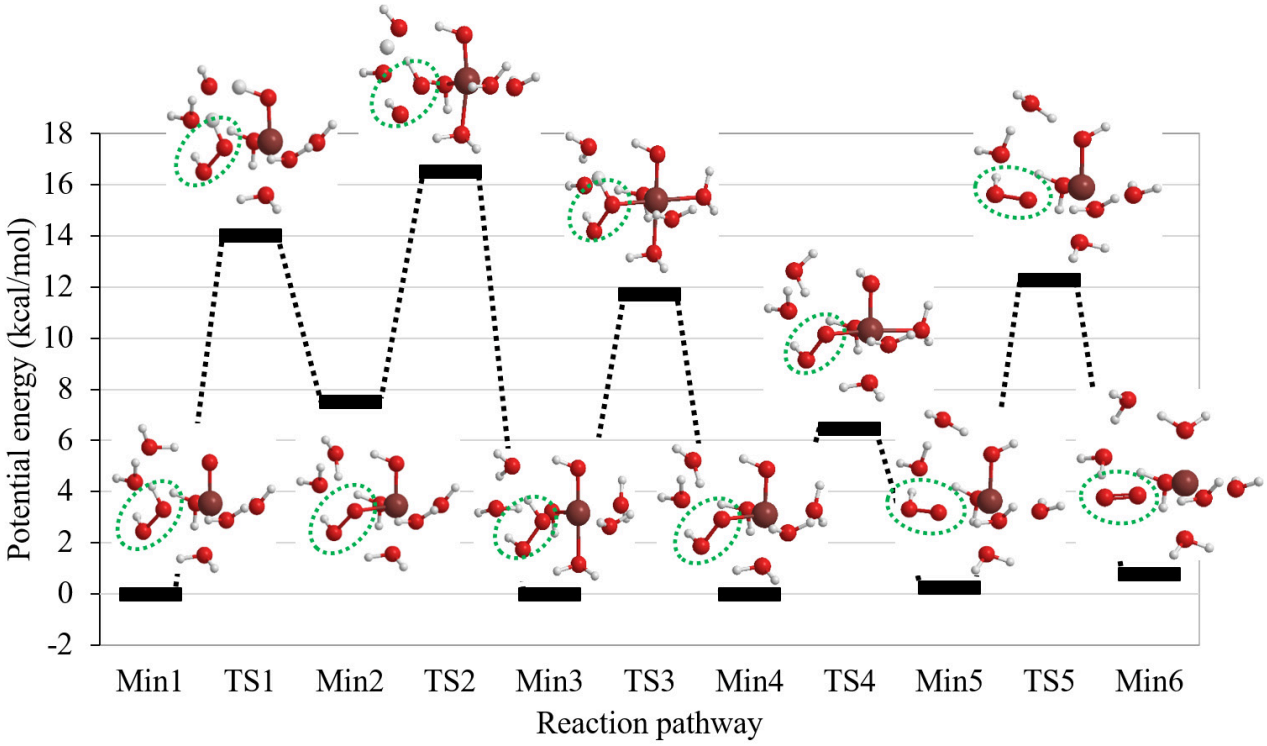

FIG. 6: O_2 formation mechanism of the H_2O_2-coordinated FeO^+ ion hydration complex with two H_2O molecules, i.e., $[FeO(H_2O_2)(H_2O)_4]^+(H_2O)_2$. LC-BLYP/cc-pVDZ/LanL2DZ is used with the solvent effect of the polarizable continuum model of water. Zero-point vibrational corrections are included. The potential energy of the reactant complex (Min1) is set to be zero. The dotted green circles indicate the H_2O_2 molecules and their decomposed fragments.

conclude that the conventional H_2O_2 decomposition mechanism, which usually contain the OH radical production, should be replaced with this new mechanism.

Finally, it is interesting to note that Fig. 5 also reveals the O_2 formation mechanism from the $[Fe(OH)_2]^+$ complex, which is obtained as a product in Eq. (22). Since Min3 in Fig. 5 corresponds to the $[Fe(OH)_2]^+$ complex coordinating H_2O_2, the O_2 formation reaction from this complex is considered to take a short cut from this Min3. This result strongly suggests that the reaction proceeds directly from the $[Fe(OH)_2]^+$ complex bypassing the FeO^+ complex formation, i.e.,

$$[Fe^{\mathrm{III}}(OH)_2(H_2O)_4]^+ \rightarrow [Fe^{\mathrm{I}}(H_2O)_6]^+ + O_2. \tag{30}$$

This figure also indicates that the FeO^+ hydration complex is formed from the $[Fe(OH)_2]^+$ complex with the reaction barrier of 16.5 kcal/mol in the backward process from Min3

through Min1, while this barrier is small enough to initiate the reaction at room temperature as mentioned in Sec. III B. We, therefore, propose that this H_2O_2 decomposition mainly proceeds through the $[Fe(OH)_2]^+$ complex with forming the FeO^+ hydration complex as a by-product, though the decomposition reaction may also partly proceed from this FeO^+ complex.

IV. CONCLUSIONS

In this study, we have theoretically explored the H_2O_2 decomposition mechanisms under the absence and presence of Fe ions in aqueous solution, following recent experimental studies on this topic. We have consequently revealed the H_2O_2 decomposition mechanisms, which contain no OH radical formations as supported by the experimental results.

We first addressed the H_2O_2 decomposition under the absence of metal ions in aqueous solution. As a test, we calculated the O-O dissociation potential energy curves of H_2O_2 with several numbers of explicitly-hydrated water molecules in the solvent model of water, under the spin-stability conditions for switching the spin-restricted and -unrestricted Kohn-Sham calculations. The calculated results show that although the O-O dissociation potentials asymptotically approach the energies of OH radicals, they essentially require the spin-forbidden transitions. We, therefore, presumed an H_2O_2 decomposition mechanism using H_2O_2 dimer and calculated the reaction energy diagrams for several hydration numbers. As a result, we found that this mechanism provides reasonable barrier heights (52 $\sim$ 62 kcal/mol), which are close to the experimentally-evaluated activation energy (47.8 kcal/mol). We, therefore, conclude that this is the H_2O_2 decomposition mechanism under the absence of metal ions.

Next, we explored the H_2O_2 decomposition under the presence of Fe ions in aqueous solution. Following a recent experimental study,[10] we calculated the O-O dissociation potential energy curves of H_2O_2 coordinating to the Fe ion hydration complex to produce the FeO hydration complex. As a result, we surprisingly found that the monovalent Fe ion hydration complex, $[Fe(H_2O_2)(H_2O)_5]^+$, has no reaction barrier for the dissociation of H_2O_2, while the ferrous (Fe^{2+}) and ferric (Fe^{3+}) ion hydration complexes have very high reaction barriers. We also found that the Fe hydroxide $Fe(OH)_2^+$ ion hydration complex is first produced, and then, it is transformed into the FeO^+ ion hydration complex. We have turned up several

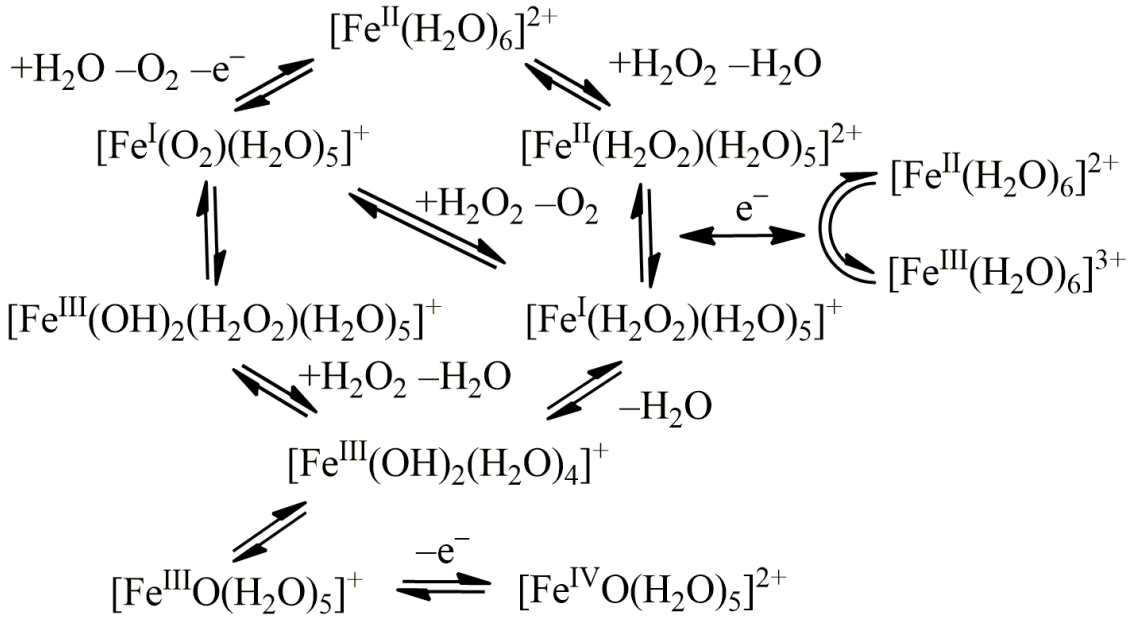

FIG. 7: Schematic overview of H_2O_2 decomposition mechanism by iron ion hydration complex.

experimental evidences supporting this finding and have theoretically discussed its validity.

Based on this result, we investigated the subsequent O_2 formation mechanism after the FeO^+ hydration complex formation. We calculated the reaction energy diagram of this formation reaction for the FeO^+ complex with no hydrogen bond network around the coordinating H_2O_2 molecule. The calculated diagram shows that this reaction provides a high barrier (39.3 kcal/mol) for the hydrogen transfer between the oxygen atoms of H_2O_2. We, therefore, attached two hydration water molecules to H_2O_2 to model the hydrogen bond network. As a result, we found that the highest barrier height dramatically decreases to 14.0 kcal/mol indicating that this reaction proceeds even at room temperature as experimentally observed. We also found that the O_2 formation reaction has a short cut from the $Fe(OH)_2^+$ complex and the FeO complex is considered to be a by-product of this reaction. The overall mechanism of the H_2O_2 decomposition reaction by Fe ion hydration complex is illustrated in Fig. 7. We, therefore, conclude that the H_2O_2 decomposition under the presence of Fe ions is driven by the electron transfer to the Fe ion hydration complex, and proceeds by the assistance of the hydrogen transfers in the hydrogen bond network around H_2O_2. This indicates that electron transfers from other complexes and hydrogen transfers through surrounding hydrogen bond network play a crucial role in the catalytic reactions of metal complexes.

ACKNOWLEDGMENTS

This research was supported by the Superlative, Stable, and Scalable Performance Fuel Cell (SPer-FC) project of the New Energy and Industrial Technology Development Organization (NEDO) and by the Japanese Ministry of Education, Culture, Sports, Science and Technology (MEXT) (Grants: 17H01188 and 16KT0047). This study was also partly supported by MEXT as "Priority Issue on Post-K computer" (Development of new fundamental technologies for high-efficiency energy creation, conversion/storage and use).

SUPPLEMENTARY MATERIAL AVAILABLE

The molecular structures of H_2O_2 decomposition reaction at each step for the explicit hydration numbers of $\lambda = 2, 4, 6$ and 8 have been provided in Fig. S1. The calculated vibrational spectra of OHOHO and HOOOH radicals, which are coordinated by two H_2O molecules, have also been given in Fig. S2. This material is available free of charge via the Internet at xxxx.

FIGURE CAPTIONS

Fig. 1.

Calculation models of (a) hydrated H_2O_2 monomer with λ hydration water molecules ($[(H_2O_2)_2(H_2O)_\lambda]$), (b) hydrated H_2O_2 dimer with λ hydration water molecules ($[(H_2O_2)_2(H_2O)_\lambda]$), (c) iron ion ($Fe^{n+}$) hydration complexes with λ coordinating water molecules ($[Fe(H_2O_2)(H_2O)_5]^{n+}$), and (d) iron oxide ion (FeO^{n+}) hydration complexes with λ coordinating water molecules and two additional water molecules ($[FeO(H_2O_2)(H_2O)_5]^{n+}(H_2O)_2$).

Fig. 2

Potential energy curves of the O-O dissociation of H_2O_2 to OH radicals for the explicit hydration numbers $\lambda = 0$, 2, 4, 6, and 8 in aqueous solution. The spin-restricted Kohn-Sham calculations are performed under the stability condition for switching to the spin-unrestricted ones.[29,30] LC-BLYP/cc-pVDZ is used with the solvent effect of the polarizable continuum model of water. The minimum potential energies are set to be zero. The dissociation limit energies, which are calculated by equally dividing the hydrated H_2O_2 such as $H_2O_2(H_2O)_{2\lambda}$ $\rightarrow 2OH(H_2O)_\lambda$, are also shown at the infinite O-O distance.

Fig. 3.

Reaction diagrams of H_2O_2 decomposition reaction, i.e., $2H_2O_2 \rightarrow O_2 + 2H_2O$, under the absence of metal ions in aqueous solution. LC-BLYP/cc-pVDZ is used with the solvent effect of the polarizable continuum model of water. Zero-point vibrational corrections are included. The molecular structures of the reaction processes are also shown for the complex with no water molecule. For Min3, the potential energy of the triplet state for $\lambda = 8$ is also shown as a black bar.

Fig. 4.

Potential energy curves of the O-O bond dissociation of H_2O_2, which is coordinated to the iron ion hydration complexes in $[Fe(H_2O_2)(H_2O)_5]^{n+}$, for the valence of $n = 1$, 2, and 3. LC-BLYP/cc-pVDZ/LanL2DZ is used with the solvent effect of the polarizable continuum model of water. The dotted green circles indicate the H_2O_2 molecule and formed H_2O molecule and OH radical.

Fig. 5.

O_2 formation mechanism of the H_2O_2-coordinated FeO^+ ion hydration complex with no additional H_2O molecules, i.e., $[FeO(H_2O_2)(H_2O)_4]^+$. LC-BLYP/cc-pVDZ/LanL2DZ is used with the solvent effect of the polarizable continuum model of water. Zero-point vibrational corrections are included. The potential energy of the reactant complex (Min1) is set to be zero. The dotted green circles indicate the H_2O_2 molecules and their decomposed fragments.

Fig. 6.

O_2 formation mechanism of the H_2O_2-coordinated FeO^+ ion hydration complex with two H_2O molecules, i.e., $[FeO(H_2O_2)(H_2O)_4]^+(H_2O)_2$. LC-BLYP/cc-pVDZ/LanL2DZ is used with the solvent effect of the polarizable continuum model of water. Zero-point vibrational corrections are included. The potential energy of the reactant complex (Min1) is set to be zero. The dotted green circles indicate the H_2O_2 molecules and their decomposed fragments.

Fig. 7.

Schematic overview of H_2O_2 decomposition mechanism by iron ion hydration complex.

* Electronic address: ttsuneda@yamanashi.ac.jp

[1] Bishop DF, Stern G, Fleischman M, Marshall LS. I&EC Process Design and Development. 1968;7:110–117.

[2] Walling C, Goosen A. J Am Chem Soc. 1973;95:2987–2991.

[3] Fenton HJH. J Chem Soc Trans. 1894;65:899–910.

[4] Haber F, Weiss J. Proc R Soc London A. 1934;147:332–351.

[5] Takagi J, Ishigure K. Nucl Sci Eng. 1985;89:177–186.

[6] Barb WG, Baxendale JH, George P, Hargrave KR. Reactions of ferrous and ferric ions with hydrogen peroxide. Part I. The ferrous ion reaction. Trans Faraday Soc. 1951;42:155–169.

[7] Walling C, Weil T. Int J Chem Kinet. 1974;6:507–516.

[8] Bray WC, Gorin MH. Ferryl ion, a compound of tetravalent iron. J Am Chem Soc. 1932;54:2124–2125.

[9] Buda F, Ensing B, Gribnau MCM, Baerends EJ. DFT Study of the Active Intermediate in the Fenton Reaction. Chem Eur J. 2001;7:2775–2783.

[10] Enami S, Sakamoto Y, Colussi AJ. Proc Nat Acad Sci. 2014;111:623–628.

[11] Kohn W, Sham LJ. Phys Rev A. 1965;140:1133–1138.

[12] Tsuneda T. Density Functional Theory in Quantum Chemistry. Tokyo: Springer; 2014.

[13] Tsuneda T, Hirao K. WIREs Comput Mol Sci. 2014;4:375–390.

[14] Iikura H, Tsuneda T, Yanai T, Hirao K. A long-range correction scheme for generalized-gradient-approximation exchange functionals. J Chem Phys. 2001;115(8):3540–3544.

[15] Becke AD. Phys Rev A. 1988;38:3098–3100.

[16] Lee C, Yang W, Parr RG. Development of the Colle-Salvetti correlation-energy formula into a functional of the electron density. Phys Rev B. 1988;37:785–789.

[17] Tawada Y, Tsuneda T, Yanagisawa S, Yanai T, Hirao K. J Chem Phys. 2004;120:8425–8433.

[18] Tsuneda T, Singh RK, Iiyama A, Miyatake K. ACS Omega. 2017;2:4053–4064.

[19] Tsuneda T, Miyake J, Miyatake K. ACS Omega. 2018;3:259–265.

[20] Dunning Jr TH. Gaussian basis sets for use in correlated molecular calculations. I. The atoms boron through neon and hydrogen. J Chem Phys. 1989;90:1007–1023.

[21] Kendall RA, Dunning JTH, Harrison RJ. Electron affinities of the first-row atoms revisited.

Systematic basis sets and wave functions. J Chem Phys. 1992;96:6796–6806.

[22] Hay PJ, Wadt WR. J Chem Phys. 1985;82:299–310.

[23] Tomasi J, Mennucci B, Cammi R. Chem Rev. 2005;105:2999–3093.

[24] Peng C, Schlegel HB. Combining Synchronous Transit and Quasi - Newton Methods to Find Transition States. Israel J Chem. 1993;33:449–454.

[25] Peng C, Ayala PY, Schlegel HB, Frisch MJ. Using redundant internal coordinates to optimize equilibrium geometries and transition states. J Comput Chem. 1996;17:49–56.

[26] Maeda A, Harabuchi Y, Ono Y, Taketsugu T, Morokuma K. Int J Quantum Chem (Special Issue: Theoretical Chemistry in Japan). 2015;115:258–269.

[27] Hratchian HP, Schlegel HB. Accurate reaction paths using a Hessian based predictor-corrector integrator. J Chem Phys. 2004;120:9918–9924.

[28] Hratchian HP, Schlegel HB. Using Hessian updating to increase the efficiency of a Hessian based predictor-corrector reaction path following method. J Chem Theory Comput. 2005;1:61–69.

[29] Bauernschmitt R, Ahlrichs R. Chem Phys Lett. 1996;256:454–464.

[30] Seeger R, Pople JA. J Chem Phys. 1977;66:3045–3050.

[31] Frisch MJ, Trucks GW, Schlegel HB, Scuseria GE, Robb MA, Cheeseman JR, et al.. Gaussian09 Revision D.01; 2009. Gaussian Inc. Wallingford CT.

[32] Dennington R, Keith T, Millam J. GaussView, Version 5; 2009. Semichem Inc., Shawnee Mission KS.

[33] Hiroki A, LaVerne JA. J Phys Chem B. 2005;109:3364–3370.

[34] Giguerre PA, Liu ID. Can J Chem. 1957;35:283–293.

[35] Kijewski H, Troe J. Int J Chem Kinet. 1971;3:223–235.

[36] Tessier A, Forst W. Can J Chem. 1974;52:794–797.

[37] Baulch DL, Cobos CJ, Cox RA, Frank P, Hayman G, Just T, et al. J Phys Chem Ref Data. 1994;23:847.

[38] Gray P. Trans Faraday Soc. 1959;55:408–417.

[39] De Laat J, Gallard H. Environ Sci Technol. 1999;33:2726–2732.

[40] Evans RW, Rafique R, Zarea A, Rapisarda C, Cammack R, Evans PJ, et al. J Biol Inorg Chem. 2008;13:57–74.

[41] Nishida Y. The Chemical Times (Japanese). 2015;236:8–16.

[42] Marcus RA. Rev Mod Phys. 1993;65:599–610.

[43] Chandler D. Electron transfer in water and other polar environments, how it happens. In: Berne BJ, Ciccotti G, Coker DF, editors. Classical and Quantum Dynamics in Condensed Phase Simulations. Singapore: World Scientific; 1998. p. 25–49.